Article

Polymorph Selection of ROY by Flow-Driven Crystallization

Iwona Ziemecka [1,2,*], **Sindy Gokalp** [1], **Sander Stroobants** [3], **Fabian Brau** [1],
Dominique Maes [3] **and Anne De Wit** [1,*]

1   Nonlinear Physical Chemistry Unit, Université libre de Bruxelles (ULB), 1050 Brussels, Belgium
2   μFlow Group, Department of Chemical Engineering, Vrije Universiteit Brussel, 1050 Brussels, Belgium
3   Structural Biology Brussels, Vrije Universiteit Brussel, 1050 Brussels, Belgium
*   Correspondence: adewit@ulb.ac.be (A.D.); iwona.ziemecka@vub.be (I.Z.);
    Tel.: +3226505774 (A.D.); +3226291057 (I.Z.)

Abstract: The selection of polymorphs of the organic compound 5-methyl-2-[(2-nitrophenyl)amino]-3-thiophenecarbonitrile, ROY, is studied experimentally in the confined space between two horizontal glass plates when an acetone solution of ROY of variable concentration is injected at a variable flow rate into water. Depending on the local concentration within the radial flow, a polymorph selection is observed such that red prisms are favored close to the injection center while yellow needles are the preferred polymorph close to the edge of the injected ROY domain. At larger flow rates, a buoyancy-driven instability induces stripes at the outer edge of the displacement pattern, in which specific polymorphs are seen to crystallize. Our results evidence the possibility of a selection of ROY polymorph structures in out-of-equilibrium flow conditions.

1. Introduction

Crystallization, which is a phase transition from a solution to a highly structured solid form called a crystal, typically occurs via two specific events. First, atoms or molecules cluster together on a microscopic scale in a process called nucleation. Then, if the clusters become stable and sufficiently large, crystal growth occurs. Atoms and compounds can generally form more than one crystal structure. The ability of a molecule to adopt at least two different arrangements in the solid state is called polymorphism [1]. This arrangement of particles is determined during the nucleation stage of crystallization [2–4]. Polymorph selection may be influenced by multiple factors like temperature, pressure, concentration or even flow [5,6]. Different crystal structures of a given compound can lead to different physical and chemical properties [7]. By structure, we mean the internal arrangement of atoms, ions or molecules in crystal lattices.

One of the criteria to classify a solid material as polymorphic is its ability to exist in two or more form of crystal structure. Polymorphism must be controlled to produce drugs, pigments, explosives, etc. to avoid differences in the properties and performances of the products [8]. In the pharmaceutical field, the effects of polymorphism are the most critical as the presence of a non-desired polymorph in a mixture can affect stability, solubility, physiological activity or bioavailability of the active ingredients [9,10]. Flows play an important role during the production of crystals of pharmaceutical compounds. It remains however difficult to estimate the flow levels and associated shear stresses that are experienced during the downstream processing, filling and even shipment as well as their influence on polymorph selection.

Among all the compounds that have many polymorphs, 5-methyl-2-[(2-nitrophenyl)amino]-3-thiophenecarbonitrile (Figure 1) is particularly interesting as a model system for studies on polymorphism. Though this molecule was first synthesized by medicinal chemists as a precursor for the antipsychotic drug olanzapine, it became noticeable not for its pharmaceutical effects but for its solid-state properties. It is known to crystallize into at least ten different polymorphs out of which eight have a crystalline structure resolved in the Cambridge Structural Database [11–13]. It is also commonly called ROY, an acronym based on the first letters of "Red, Orange, Yellow" because some of its polymorphs are red, orange or yellow which makes them easy to discriminate [11,14]. Even though ROY has not more polymorphs on record than water or silica, ROY is extraordinary because the majority of its polymorphs are thermodynamically stable under the same conditions at ambient pressure and temperature and they can crystallize from the same liquid. Six polymorphs of ROY coexist at room temperature: red prisms (R), yellow prisms (Y), orange needles (ON), orange plates (OP), yellow needles (YN), and orange-red plates (ORP). They are presented in Figure 1. The seventh polymorph, red plates (RPL) crystallizes from vapor on succinic acid [15]. Two other known polymorphs are named Y04 and YT04 [16]. Y04 is a metastable polymorph obtained from a melt crystallization and it transforms to YT04 [16]. Red polymorph R05 was also obtained from pure melt ROY due to cross-nucleation on Y04.
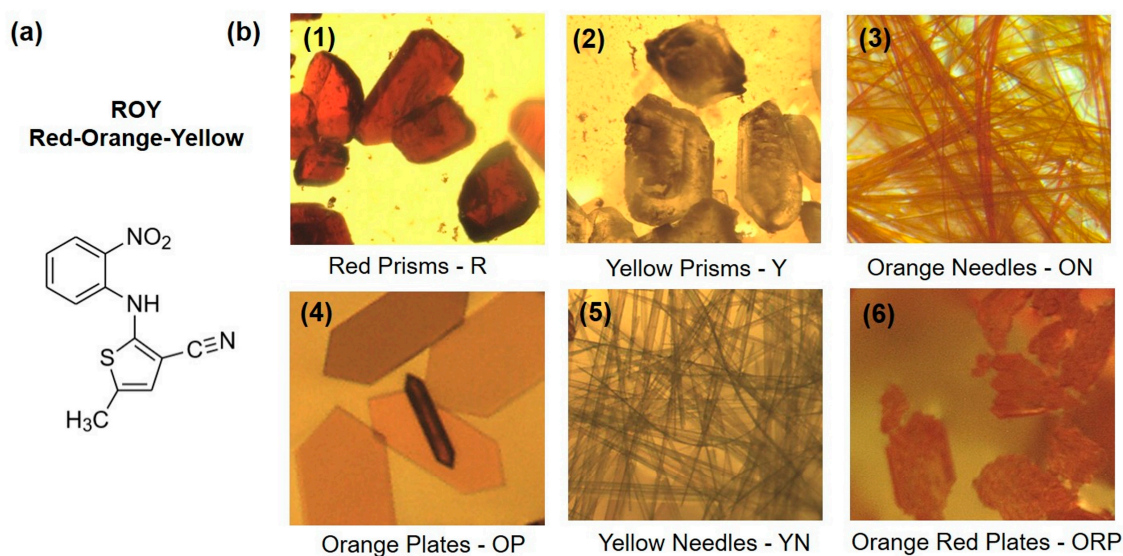

Figure 1. (**a**) Molecule of ROY, (**b**) Polymorphs of ROY: (**1**) Red Prisms—R, (**2**) Yellow Prisms—Y, (**3**) Orange Needles—ON, (**4**) Orange Plates—OP, (**5**) Yellow Needles—YN, (**6**) Orange Red Plates—ORP.

The colored properties of ROY make it an ideal model substance for studying the influence of a flux in the crystallization process. The aim of this work is to study the crystallization of these polymorphs during a radial injection of an acetone solution of ROY into water in a quasi-two-dimensional geometry of a Hele-Shaw cell (two glass plates separated by a thin gap). It has indeed recently been shown that precipitation occurring in the presence of such a hydrodynamic flow could generate thermodynamically unstable products [5,6]. In this context, our goal is to understand how such flow conditions influence the crystallization and selection of ROY polymorphs.

To achieve this, we will use as an experimental system a Hele-Shaw cell where an acetone solution of ROY is injected at a given flow rate in water initially at rest. This cell is used to study out-of-equilibrium dynamics by confining the system between two transparent plates, thus reducing one spatial dimension in order to easily analyze the patterns obtained and potential hydrodynamic instabilities caused by the injection of one fluid into another. These hydrodynamic instabilities are generated if the two fluids have significantly different densities and/or viscosities [17–20]. Density differences lead to buoyancy-driven instabilities in the form of small stripes at the edge of the displacement [17]. Unequal viscosities can in some cases trigger a viscous fingering instability [19,20].

It has recently been shown that the interaction between precipitation reactions and such hydrodynamic instabilities produces a wealth of precipitation patterns and crystalline structures that can be significantly different from those obtained in well-mixed homogeneous reactors [5,6,18–25]. It is even possible to favor the product of thermodynamically unstable composition, as has been shown in the calcium-oxalate [5,23] and the calcium-carbonate [24] systems.

In this work, we demonstrate that, out-of-equilibrium, flow-driven precipitation in the confined space of a Hele-Shaw cell can lead to selective production of the various ROY polymorphs. First, the methodology and operating procedures of equilibrium crystallization experiments are presented. An experimental study of equilibrium crystallization is carried out to establish the diagram of polymorphs at equilibrium as a function of the solvent/antisolvent ratio and the concentration of ROY. An out-of-equilibrium study in a Hele-Shaw cell is then performed under flow conditions and various patterns are obtained when the ROY concentration and flow rate are varied. To conclude, the results of in-equilibrium and out-of-equilibrium experiments will be compared to study the effect of flow on the crystallization of ROY and on the selection of polymorphs.

2. Materials and Methods

2.1. General

ROY, 5-methyl-2-[(2-nitrophenyl)amino]-3-thiophenecarbonitrile, was purchased from Toronto Chemical Research. ROY solutions of concentrations 10, 25, and 50 mg/mL (of density 0.796, 0.801 and 0.812 g/mL, respectively) were prepared by dissolving ROY in acetone (Acros Organics, purity > 99%). Ultrapure water with a density of 1.000 g/mL was used as an antisolvent. The density of the solutions was determined by an Anton Paar DMA 35N densitometer (Anton Paar GmbH, Graz, Austria). The viscosity of pure acetone and of the most concentrated 50 mg/mL ROY solution in acetone, measured using Dynamic Light Scattering, is 0.355 and 0.845 mPa·s respectively.

2.2. Phase Diagrams

Crystallization was performed in 48 Well Plates (VDX, Hampton Research). Varying volumes of a ROY acetone solution at concentration of 10, 25, and 50 mg/mL and water were injected into each well. The liquid was mixed with a micropipette to obtain a homogeneous solution. The wells were closed with a glass lens to prevent evaporation of acetone. The multi-well plates were kept at a controlled temperature of 20 °C for a week.

2.3. Flow-Driven Crystallization in A Hele-Shaw Cell

Out-of-equilibrium experiments were performed at ambient temperature in a horizontal Hele-Shaw cell consisting of two transparent glass plates separated by a spacer of thickness 0.5 mm. The gap between the plates was filled with water as antisolvent. The ROY solution was injected from the center of the bottom plate at a constant flow rate through a valve using a syringe pump (KDS Model 200 Series) (KD Scientific Inc., Holliston, MA, USA). The studied injection flow rates were 0.2, 1 and 5 mL/min. A schematic representation of a Hele-Shaw cell is shown in Figure 2.

The dynamic images taken by a Nikon lens-coupled CCD camera were recorded from above at a frequency up to 50 fps using the Gigaviewer open-source program. The size of the images is 2048 × 1088 pixels for a field of view of 278.93 mm × 148.18 mm. A Nikon D700 camera (Nikon Corporation, Tokyo, Japan) with a Nikon ED AF Nikkor 200 mm lens 1:4 D that can take pictures up to 24 million pixels is used to distinguish the polymorphs that are formed.
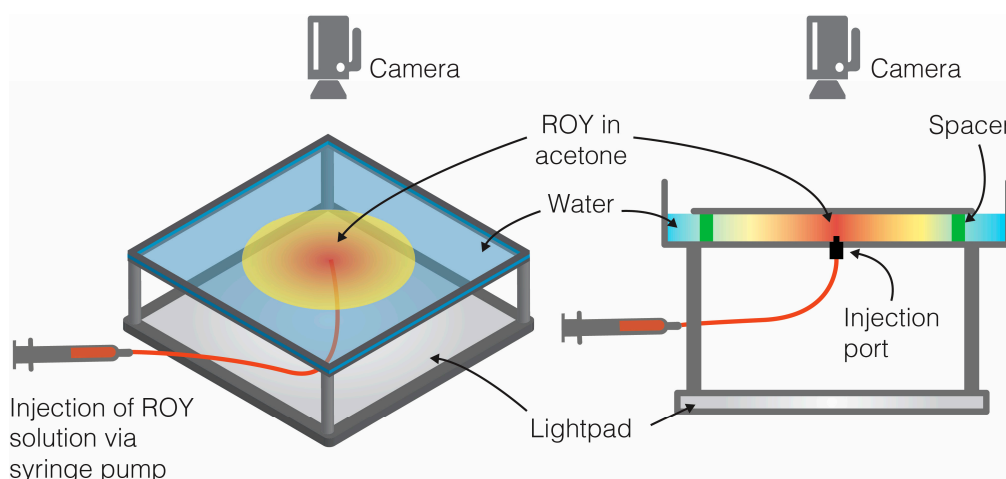
Figure 2. Schematic drawing of the experimental setup. The Hele-Shaw cell consists of two glass plates separated by a spacer of thickness 0.5 mm. The setup is illuminated from below by a lightpad. A camera is placed above the setup. Into the Hele-Shaw cell containing the water, 2 mL of an acetone solution of ROY was pumped by a syringe pump with variable flow rates of 0.2 up to 5 mL/min.

3. Results and Discussion

3.1. Equilibrium Polymorphs

In equilibrium conditions, the ROY molecule crystallizes into various polymorphs depending on the percentage of water in the total volume of solution and the initial concentration of ROY in acetone. Figure 3 gives a phase diagram identifying the various ROY polymorphs observed at equilibrium at room temperature and pressure, 96 h after the given ROY solution has been mixed in wells with water in variable content. At lower water content, the main polymorphs are red and yellow prisms. Orange plates, orange-red plates, and orange needles are the preferred structure at intermediate water percentage while orange-red plates and yellow needles are the favored polymorphs at larger water content. The three different ROY concentrations studied in the phase diagram of Figure 3 are next used to see which polymorphs are obtained when these solutions are injected into water.
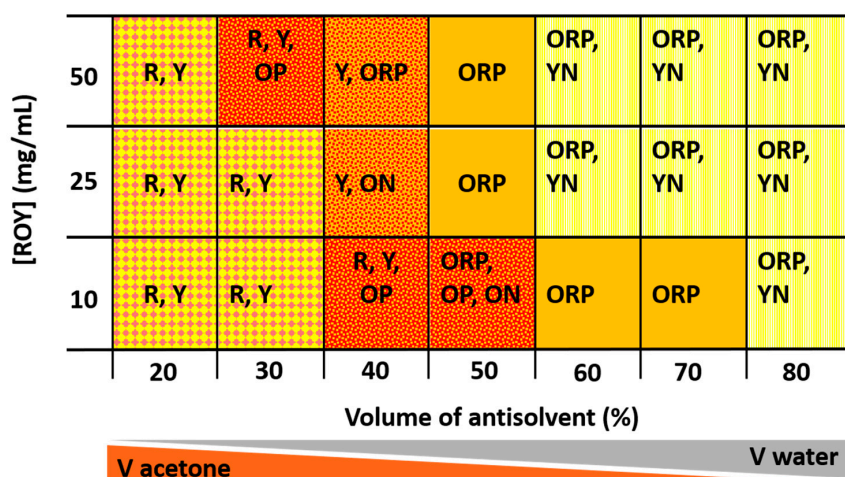

Figure 3. Equilibrium phase diagram of ROY polymorphs. The concentration indicated in the rows refers to the concentration of the acetone solution of ROY before adding the antisolvent. The percentage of antisolvent (water) in the total volume of solution is indicated in the columns. Polymorphs of ROY: Red Prisms—R, Yellow Prisms—Y, Orange Needles—ON, Orange Plates—OP, Yellow Needles—YN, Orange Red Plates—ORP.

3.2. Out-of-Equilibrium ROY Patterns

In the out-of-equilibrium experiments, the ROY solution was injected into the Hele-Shaw cell initially filled with water at a given flow rate Q and the spatial-temporal distribution of this compound was recorded. As seen in Figures 4 and 5, the precipitation patterns depend on the concentration of ROY in the injected solution and on the flow rate. Note that, in these flow conditions, the concentrations vary in space and time along the radius of injection and so does the supersaturation (SI). The exact values of SI are however not instructive as previous studies on precipitation of calcium carbonate in similar flow conditions have shown that sometimes, patterns with a very low amount of solid precipitate were obtained even if SI was very large and that patterns can change quite a lot for similar values of SI [25]. Kinetic effects can in addition also play a role. It is also impossible to perform a quantitative study of the crystals formed because they cannot be collected without opening the cell, which mixes the solutions and thus the different polymorphs, induces further precipitation and destroys some of the crystals.
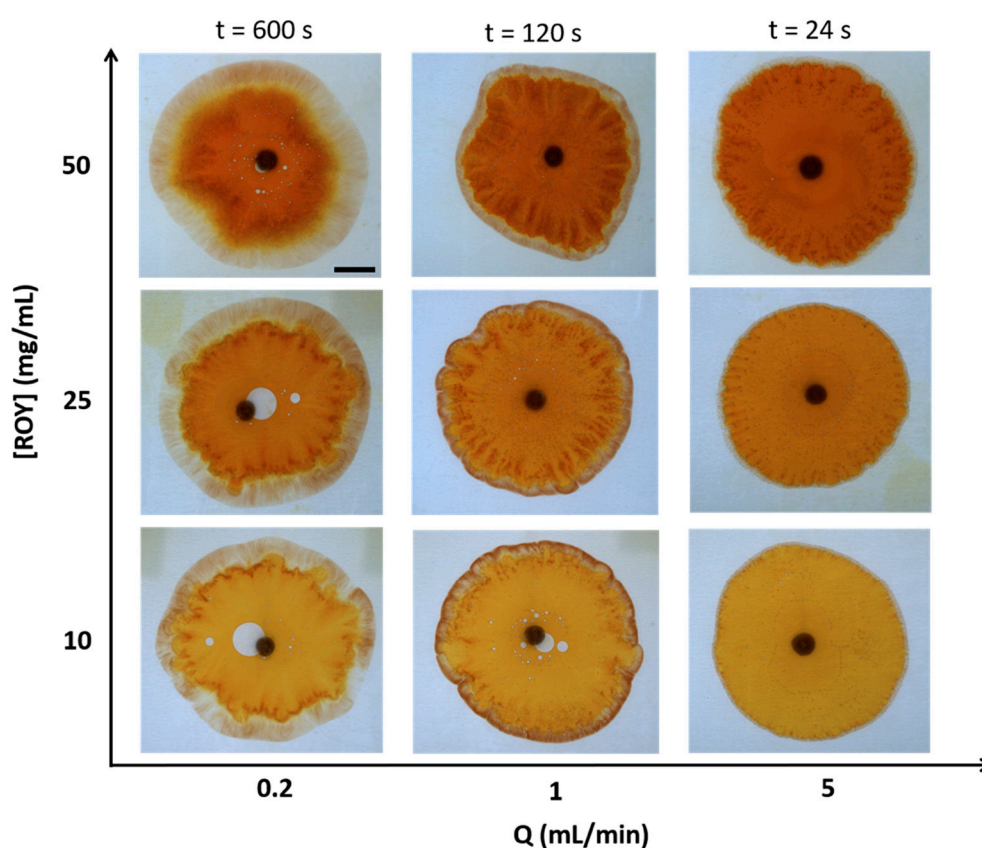

Figure 4. Precipitation patterns after injection of 2 mL of ROY acetone solution of concentration (top row) 50, (middle row) 25, and (bottom row) 10 mg/mL into the Hele-Shaw cell containing the water, at the different injection rates indicated on the horizontal axis: (left column) 0.2, (middle column) 1 and (right column) 5 mL/min. The scale bar is 1 cm.

Nevertheless, we observe that, at larger flow rates, the distribution remains mainly orange indicating low mixing between the ROY solution and water. At the lowest flow rate, a more fingered deformation of the outer zone is observed. Moreover, large zones of yellow color are obtained at the edge of the pattern because of a more diluted concentration profile. This can be rationalized in terms of the Péclet number $Pe = UL/D$ giving the ratio between the hydrodynamic advection rate and the diffusive transport rate where U is the local flow velocity, L is a characteristic length of the problem, typically the gap width of the cell, and D is the mass diffusion coefficient. At large Pe numbers, corresponding to large injection rates, advection dominates, and the concentration profile of ROY is sharply transitioning from the concentration of the injected solution to that of the pure water.

The orange ROY solution is then the main component observed in the cell with a small yellow zone at the rim. On the contrary, at low Pe, diffusion has more time to act such that the ROY concentration profile is more spatially extended and the whole range of polymorphs can unfold spatially in the system. Figure 5 also shows that the larger the ROY concentration, the more striped indentations are observed at the rim of the injected solution while the inner orange pattern is more fingered at smaller ROY concentrations. These observations will be further discussed in the next section.
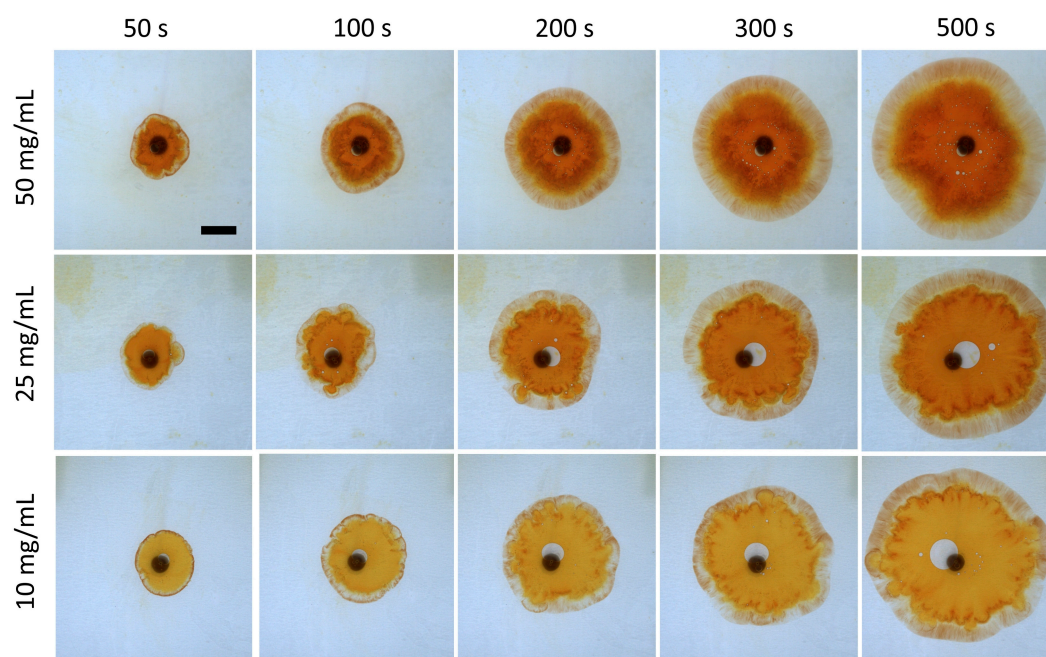

Figure 5. Spatio-temporal evolution of ROY patterns at the concentration of 10, 25, 50 mg/mL when injected into water. The scale bar is 1 cm and the injection speed 0.2 mL/min.

Interestingly, injection of the ROY solution into water causes the nucleation of bubbles of gas, as seen on the Videos in the Supplementary Materials. This can be explained by the lower gas solubility in water than in acetone [26]. Upon mixing the ROY solution with water, the local solubility of gas is decreased resulting in the formation of bubbles. At the high injection flow rate, the gas bubbles are both moving with and against the flow of the injected liquid. Remarkably, at the low injection flow rate, they move into the direction of high concentration of acetone.

3.3. Hydrodynamic Instabilities

Because of density differences between the ROY solution and water, a hydrodynamic buoyancy-driven fingering instability can develop [17]. As seen in Figure 6, this instability arises because, in the gap of the cell, the injected solution of ROY develops a parabolic Poiseuille profile (Figure 6a) due to the fact that the speed is zero at the solid boundaries (no-slip boundary condition). As a result of this, in a plane perpendicular to the plates (Figure 6b), the ROY solution is sandwiched in the middle of the two layers of water adjacent to the walls. In the upper part, the denser water layer overlies the less dense ROY solution, which is a buoyantly unstable situation in the gravity field. A Rayleigh-Taylor instability than induces convective rolls extending perpendicularly to the rim of the ROY/water miscible interface. These rolls result in stripes that can clearly be visible when zooming on the pattern close to the edge of the pattern (see Figures 6d and 7) similar to what was reported in absence of crystallization [17]. It is observed that this local convection has an influence on the orientation and local selection of polymorphs in our case. Indeed, as seen in Figures 6d and 7, yellow and orange needles align within the stripes while orange red plates are favored in the cusps of the stripes where local mixing is larger and brings more ROY solution in contact with water.

The buoyancy-driven instability and the resulting convective rolls can thus have an influence on the local selection of ROY polymorphs as seen in other systems [6,18,24].
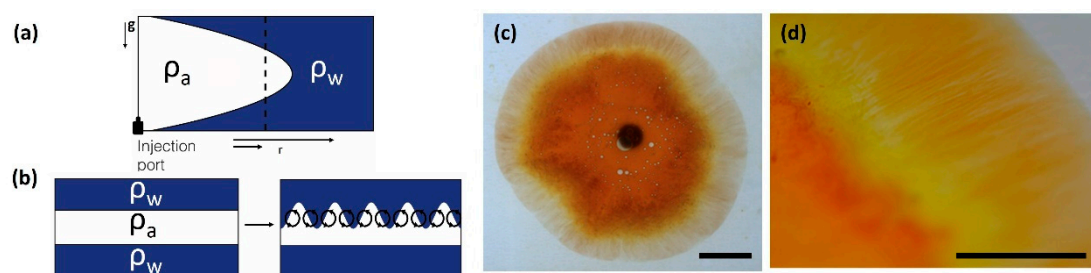

Figure 6. (**a**) Sketch of the Poiseuille profile in the gap of the cell obtained when the ROY solution of density ρ_a (white) is injected along the radius r into water of density ρ_w (blue). (**b**) Transverse cut in the gap along the dashed line in panel (a). Development of buoyancy-driven convective rolls at the upper miscible interface where the denser water overlies the less dense acetone solution of ROY. (**c**) Precipitation pattern, scale bar is 1 cm, (**d**) zoom on the outer rim of the pattern, scale bar: 0.5 cm.

Figure 7. Zoom on the edge of the displacement showing aligned yellow and orange needles in the zone of buoyancy stripes. Behind them, orange red plates develop at the locations where the local mixing due to the convection rolls (see Figure 6b) increases contact between the ROY solution and water.

Note also that the viscosity of water is 1 mPa·s while the one of pure acetone and of the most concentrated solution of ROY in acetone is 0.355 and 0.845 mPa·s respectively. Technically, we have thus a low viscosity solution which displaces a more viscous one, which is a displacement prone to give a viscous fingering instability [20]. The viscosity ratio between the two solutions is however smaller than 3 and is thus too small to give any viscous fingering instability. Indeed, Haudin et al. [19,20] have shown in a similar geometry and flow configuration that viscous fingering is active in affecting chemical garden precipitates only for a viscosity ratio of the order of 40. The fingering observed at the edge of the orange zone in Figures 5 and 8 could however be due to local changes of permeability in the cell due to the presence of solid crystals around which the injected solution flows [22]. As seen in Figure 5, when the concentration of ROY increases in the acetone solution, its viscosity could also increase which could have a stabilizing effect on the fingering due to changes in permeability. This could explain why the more concentrated pattern in Figure 5 is more circular than those at lower concentrations.

Figure 8. Example of fingered pattern at the edge of the orange zone.

4. Conclusions

We have shown here experimentally that out-of-equilibrium flow conditions can impact the crystallization of polymorphs of the ROY compound. In particular, when a solution of ROY is injected into a confined geometry containing water, the phase diagram of polymorphs can unfold spatially. The equilibrium polymorphs characteristically obtained at low water content are then seen in the inner part of the displacement while yellow and orange needles obtained at equilibrium for larger water content are unfolding at the outer rim of the flow pattern. A buoyancy-driven instability due to differences in density between the ROY solution and water is responsible for the formation of stripes at the outer edge of the pattern. Alignment of yellow and orange needles and selection of orange red plates within the stripes are then obtained. Our results evidence the possibility of selection of polymorph structures in out-of-equilibrium flow conditions. For the further understanding of this phenomenon, future works will aim at studying polymorph selection in well-defined selected flow profiles (plug flow, laminar flow, constant shear, . . .) and in microfluidic devices.

Author Contributions: Conceptualization, A.D. and D.M.; methodology, A.D. and I.Z.; software, F.B.; validation, I.Z., S.G. and S.S.; resources, A.D., D.M., F.B., I.Z., S.G. and S.S.; writing—original draft preparation, A.D., D.M., I.Z. and S.S.; writing—review and editing, A.D., D.M., I.Z. and S.S.; project administration, A.D. and D.M.; funding acquisition, A.D. and D.M.

References

1. Bernstein, J. *Polymorphism in Molecular Crystals*; Oxford University Press: Oxford, UK, 2019.
2. Vekilov, P. Nucleation. *Cryst. Growth Des.* **2010**, *10*, 5007–5019. [CrossRef] [PubMed]

3. Vorontsova, M.; Maes, D.; Vekilov, P.G. Recent advances in the understanding of two-step nucleation of protein crystals. *Faraday Discuss.* **2015**, *179*, 27–40. [CrossRef] [PubMed]

4. Nanev, C.N. Peculiarities of protein crystal nucleation and growth. *Crystals* **2018**, *8*, 422. [CrossRef]

5. Bohner, B.; Schuszter, G.; Berkesi, O.; Horváth, D.; Tóth, A. Self-organization of calcium oxalate by flow-driven precipitation. *Chem. Commun.* **2014**, *50*, 4289–4291. [CrossRef] [PubMed]

6. Tóth-Szeles, E.; Schuszter, G.; Tóth, A.; Kónya, Z.; Horváth, D. Flow-driven morphology control in the cobalt-oxalate system. *CrystEngComm* **2016**, *18*, 2057–2064. [CrossRef]

7. Chen, S.; Xi, H.; Yu, L. Cross-nucleation between ROY polymorphs. *J. Am. Chem. Soc.* **2005**, *127*, 17439–17444. [CrossRef] [PubMed]

8. Llinas, A.; Goodman, J.M. Polymorph control: Past, present and future. *Drug Discov. Today* **2008**, *13*, 198–210. [CrossRef] [PubMed]

9. Chemburkar, S.R.; Bauer, J.; Deming, K.; Spiwek, H.; Patel, K.; Morris, J.; Henry, R.; Spanton, S.; Dziki, W.; Porter, W.; et al. Dealing with the impact of ritonavir polymorphs on the late stages of bulk drug process development. *Org. Process Res. Dev.* **2000**, *4*, 413–417. [CrossRef]

10. Kryukova, M.A.; Sapegin, A.V.; Novikov, A.S.; Krasavin, M.; Ivanov, D.M. New crystal forms for biologically active compounds Part 1: Noncovalent interactions in adducts of nevirapine with XB donors. *Crystals* **2019**, *9*, 71. [CrossRef]

11. Yu, L. Polymorphism in molecular solids: An extraordinary system of red, orange, and yellow crystals. *Acc. Chem. Res.* **2010**, *43*, 1257–1266. [CrossRef]

12. Cruz-Cabeza, A.J.; Bernstein, J. Conformational Polymorphism. *Chem. Rev.* **2014**, *114*, 2170–2191. [CrossRef] [PubMed]

13. Tan, M.; Shtukenberg, A.G.; Zhu, S.; Xu, W.; Dooryhee, E.; Nichols, S.M.; Ward, M.D.; Kahr, B.; Zhu, Q. ROY revisited, again: The eighth solved structure. *Faraday Discuss.* **2018**, *211*, 477–491. [CrossRef] [PubMed]

14. Yu, L. Color changes caused by conformational polymorphism: Optical-Crystallography, single-crystal spectroscopy, and computational chemistry. *J. Phys. Chem. A* **2002**, *106*, 544–550. [CrossRef]

15. Mitchell, C.A.; Yu, L.; Ward, M.D. Selective nucleation and discovery of organic polymorphs through epitaxy with single crystal substrates. *J. Am. Chem. Soc.* **2001**, *123*, 10830–10839. [CrossRef] [PubMed]

16. Chen, S.; Guzei, I.A.; Yu, L. New polymorphs of ROY and new record for coexisting polymorphs of solved structure. *J. Am. Chem. Soc.* **2005**, *127*, 9881–9885. [CrossRef] [PubMed]

17. Haudin, F.; Riolfo, L.A.; Knaepen, B.; Homsy, G.M.; De Wit, A. Experimental study of a buoyancy-driven instability of a miscible horizontal displacement in a Hele-Shaw cell. *Phys. Fluids* **2014**, *26*, 044102. [CrossRef]

18. Schuszter, G.; Brau, F.; De Wit, A. Flow-driven control of calcium carbonate precipitation patterns in a confined geometry. *Phys. Chem. Chem. Phys.* **2016**, *18*, 25592–25600. [CrossRef] [PubMed]

19. Haudin, F.; Cartwright, J.H.E.; Brau, F.; De Wit, A. Spiral precipitation patterns in confined chemical gardens. *Proc. Natl. Acad. Sci. US* **2014**, *111*, 17363–17367. [CrossRef]

20. Haudin, F.; De Wit, A. Patterns due to an interplay between viscous and precipitation-driven fingering. *Phys. Fluids* **2015**, *27*, 113101. [CrossRef]

21. Balog, E.; Bittmann, K.; Schwarzenberger, K.; Eckert, K.; De Wit, A.; Schuszter, G. Influence of microscopic precipitate structures on macroscopic pattern formation in reactive flows in a confined geometry. *Phys. Chem. Chem. Phys.* **2019**, *21*, 2910–2918. [CrossRef]

22. Nagatsu, Y.; Ishii, Y.; Tada, Y.; De Wit, A. Hydrodynamic fingering instability induced by a precipitation reaction. *Phys. Rev. Lett.* **2014**, *113*, 024502. [CrossRef] [PubMed]

23. Bohner, B.; Endrodi, B.; Horváth, D.; Tóth, A. Flow-driven pattern formation in the calcium-oxalate system. *J. Chem. Phys.* **2016**, *144*, 164504. [CrossRef] [PubMed]

24. Bohner, B.; Schuszter, G.; Horváth, D.; Tóth, A. Morphology control by flow-driven self-organizing precipitation. *Chem. Phys. Lett.* **2015**, *631*, 114–117. [CrossRef]

25. Schuszter, G.; Brau, F.; De Wit, A. Calcium carbonate mineralization in a confined geometry. *Env. Sci. Technol. Lett.* **2016**, *3*, 156–159. [CrossRef]

26. Jodecke, M.; Perez-Salado, K.A.; Maurer, G. Experimental investigation of the solubility of CO_2 in (acetone + water). *J. Chem. Eng. Data* **2007**, *52*, 1003–1009. [CrossRef]